Electronic Supplementary Information

Electrokinetic separation of bacteriophage ϕKZ from bacterial cells

Viswateja Kasarabada,[a] Zakia Azad,[b] Julie A. Thomas,*[b] Blanca H. Lapizco-Encinas.*[a]

[a] Microscale Bioseparations Laboratory and Biomedical Engineering Department, Rochester Institute of Technology, 160 Lomb Memorial Drive, Rochester, New York, 14623, United States.

[b] Thomas H. Gosnell School of Life Sciences, Rochester Institute of Technology, Rochester, NY 14623, USA

Correspondence should be addressed to the following authors:
Julie A. Thomas (PhD)
Email: jatsbi@rit.edu

Blanca H. Lapizco-Encinas (PhD)
Email: bhlbme@rit.edu

CONTENTS

S1. EVALUATION OF THE ELECTROPHORETIC VELOCITY IN THE WEAK AND MODERATE FIELD REGIMES (INCLUDES TABLES S1 & S2) 2

S2. CONCENTRATION OF THE PARTICLES USED IN THIS STUDY (INCLUDING TABLE S3): 3

S3. COMPUTATIONAL MODEL INFORMATION (INCLUDES FIGURES S1 & S2, AND TABLES S4 & S5) 3

S4. RETENTION TIMES TABLES FOR SEPARATIONS (INCLUDING TABLE S6 AND FIGURE S3): 5

S5. CONTRIBUTIONS OF INDIVIDUAL EK PHENOMENA TOWARDS THE OVERALL VELOCITY OF THE PARTICLES (INCLUDES FIGURE S4): 8

S6. ELUTION BEHAVIOR AND STREAMING SEPARATIONS (INCLUDES VIDEOS S1–S4): 10

REFERENCES 10

S1. Evaluation of the electrophoretic velocity in the weak and moderate field regimes (includes Tables S1 & S2)

Three dimensionless parameters, namely, the dimensionless field strength coefficient (β), the Dukhin number (Du) and the Peclet number (Pe) are used to characterize the electrophoretic velocity regime of a particle under an applied electric field.[1–3] The determined regimes would then be used to calculate their respective electrophoretic mobilities; weak for linear electrophoresis (E) and moderate for nonlinear electrophoresis with cubic dependence (E^3), and strong for nonlinear electrophoresis with 3/2 dependence ($E^{3/2}$). **Tables S1** and **S2** list the values of the three dimensionless parameters, which were determined at the same voltages as the electrophoretic mobilities. The average electric field present in the channel ranges from 194.3 V/cm to 580.6 V/cm, which are well within the linear and cubic dependence regimes. The values of the three parameters for bacteriophage ϕKZ, microparticle P1, and bacteria *Escherichia coli* confirm the validity of electric field dependence

model used for the calculation of electrophoretic mobilities.

Table S1. Values of the parameters used for investigating the weak field regime representing linear dependence (E_1).

Particle ID	β	Du	Pe	E for estimating parameters (V/cm)
ϕKZ	0.03	1.54	0.01	75
P1	0.19	0.09	0.01	75
E. coli	0.35	0.04	0.01	75

Table S2. Values of the parameters used for investigating the moderate field regime representing cubic dependence (E_3).

Particle ID	β	Du	Pe	E for estimating parameters (V/cm)
ϕKZ	0.61	1.54	0.33	1500
P1	1.55	0.09	0.56	600
E. coli	2.79	0.04	1.49	600

S2. Concentration of the particles used in this study (including Table S3):

Included below are the concentrations of the particles used in the particle tracking velocimetry (PTV) experiments as well as the ratio in which they are injected into the microchannel for the separation studies.

Table S3. Base concentrations and ratios of the particles in separations.

Particle ID	Base Concentration	Ratio in the separations of ϕKZ and P1	Ratio in the separations of ϕKZ and *E. coli*
ϕKZ	2.0 x 10^{11} pfu/mL	3	3
P1	2.3 x 10^{8} particles/mL	1	N/A
E. coli	1.2 x 10^{9} cells/mL	N/A	1

S3. Computational model information (includes Figures S1 & S2, and Tables S4 & S5)

A numerical simulation was developed in COMSOL Multiphysics® to determine the electric potential distribution within the T-cross iEK microchannel. The channel geometry was designed in AUTOCAD® and imported into the simulation environment as a DXF file. The model incorporated the physical properties of the buffer solution and key boundary conditions, including the weak conductivity of the polydimethylsiloxane (PDMS) channel structure and the application of electric potentials at the channel terminals. Parameters derived from prior experimental characterization were used as inputs for the model. **Figure S1** illustrates domain and boundary conditions used in

the computational model, while **Figure S2** illustrates the cutlines employed to calculate predicted retention times ($t_{R,p}$). **Tables S4** and **S5** illustrate the equations and conditions employed for the COMSOL model.

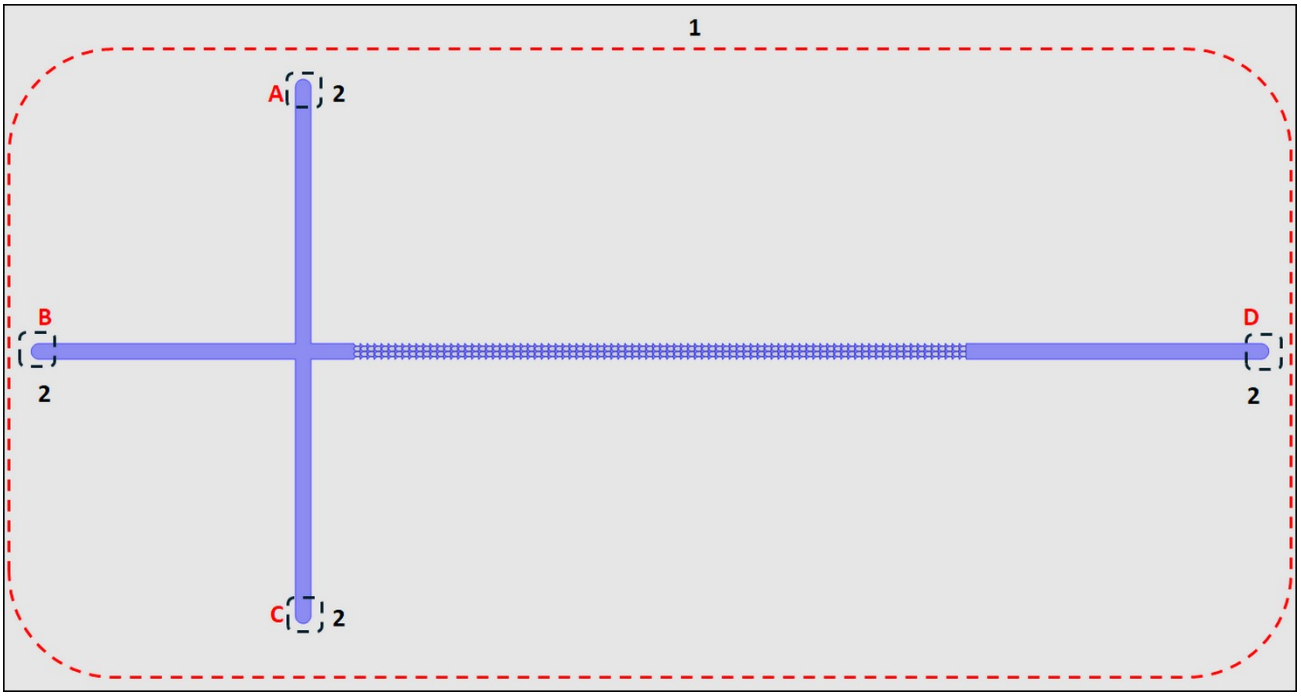

Figure S1. Schematic of the computational model's domains and boundary conditions. The model domains are color-coded: PDMS substrate (gray) and suspending medium (blue). Platinum electrodes are represented by squares within the black-dotted outlines, which also indicate the boundaries for applying electric potential. Labels A, B, C, and D denote the electrodes used for the electrokinetic (EK) injection process, corresponding to the configuration in **Table 2** of the manuscript. Refer to **Figure 1** for device dimensions and **Table S4** and **S5** for a complete list of boundary conditions. The numbered labels indicate specific boundaries detailed in **Table S4**: (1) the external PDMS surface and (2) the four reservoirs where electric potentials are applied.

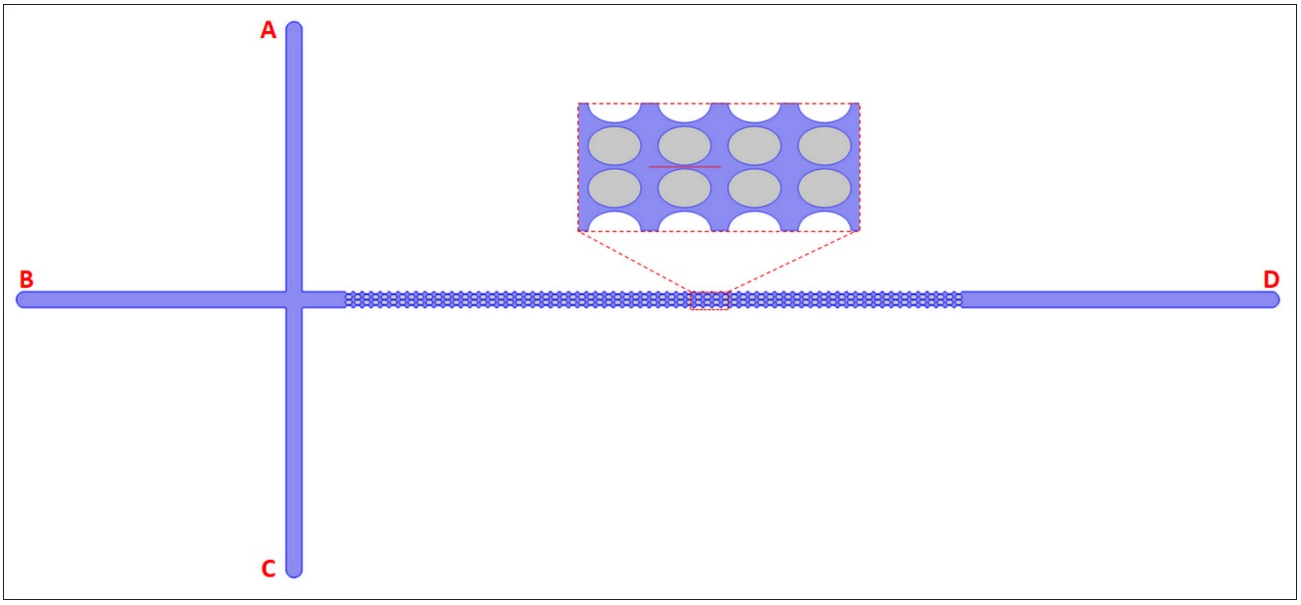

Figure S2. Representation of cutlines employed for both binary separations along with the post shapes employed in the COMSOL model to

compute the predicted retention times ($t_{R,p}$).

Table S4. Summary of the domain specifications and boundary conditions implemented in the COMSOL Multiphysics® model.

Domain conditions		
Domain type	**Element region & color**	**Definition***
Current conservation	PDMS domain (channel walls and insulating posts), gray color Fluid suspending medium domain, blue color Platinum electrodes domain, black color	$\nabla \cdot J = -\nabla \cdot \left(\left(\sigma + \varepsilon_0 \varepsilon_r \frac{\partial}{\partial t}\right) E\right)$; where $E = -\nabla \varphi$
Initial values	PDMS domain (channel walls and insulating posts), gray color Fluid suspending medium domain, blue color Platinum electrodes domain, black color	$\varphi_0 = 0$
Boundary conditions		
Boundary condition type	**Element number**	**Definition**
Electric insulation	1	$n \cdot J = 0$
Electric potential	2	$\varphi_A = \varphi_{applied,A}$; $\varphi_B = \varphi_{applied,B}$; $\varphi_C = \varphi_{applied,C}$; $\varphi_D = \varphi_{applied,D}$;

* In this table, φ represents the electric potential, J is the electric current. The variables ε_0 and ε_r represent the permittivity of the vacuum and the relative permittivity of the fluid suspending medium, respectively. The permittivity of the fluid suspending medium is $\varepsilon_m = \varepsilon_0 \varepsilon_r$.

* In this model, PDMS is not assumed to be a perfect insulator; instead, the properties of PDMS, as shown in **Table S5** below, are incorporated.

Table S5. Properties of PDMS included in the COMSOL simulation.

PDMS properties	**Value**	**Units**
Electrical conductivity	2.5 x 10^{-14}	S/m
Dielectric constant (Permittivity)	2.3-2.8	-

S4. Retention times tables for separations (including Table S6 and Figure S3):

The predicted retention times ($t_{R,p}$) were computed using the COMSOL model at the voltages selected, *i.e.,* V_A = 100 V, V_B = 700 V, V_C = 100 V, and V_D = 0 V were used to compute the electric field distribution across the channel. The average value of electric field inside the post array was computed to be 194.3 V/cm as shown in **Figure S3**.

Table S6. COMSOL predicted retention times ($t_{R,p}$) for phage ϕKZ, microparticles and *E. coli* with respect to voltage applied in reservoir B (V_B). For all the results, V_A = 100 V, V_C = 100 V and V_D = 0 V.

Sim #	V_B (V)	$t_{R1,p}$ (s) (ϕKZ)	$t_{R2,p}$ (s) (P1)	$t_{R3,p}$ (s) (*E. coli*)	$\Delta t_{R,p,1} = t_{R3,p} - t_{R1,p}$ (s)	$\Delta t_{R,p,2} = t_{R1,p} - t_{R2,p}$ (s)
1	400	361.4	190.7	179.6	180.3	169.2
2	500	310.2	163.8	154.5	154.4	145.1
3	600	271.8	143.6	135.7	134.9	127.0
4	**700**	**241.8**	**127.9**	**121.0**	**119.7**	**112.8**
Voltage at V_B selected for linear separations						
5	800	217.8	115.3	109.3	107.5	101.5
6	900	198.2	105.0	99.8	97.4	92.2
7	1000	181.8	96.5	91.9	88.9	84.4
8	1100	167.9	89.2	85.3	81.8	77.8
9	1200	156.1	83.0	79.6	75.5	72.1
10	1300	145.8	77.7	74.8	70.1	67.2
11	1400	136.7	73.0	70.6	65.3	62.9
12	1500	128.8	68.9	66.9	61.0	59.0
13	1600	121.7	65.2	63.8	57.1	55.6
14	1700	115.4	62.0	61.0	53.5	52.5
15	**1800**	**109.7**	**59.1**	**58.7**	**50.2**	**49.8**
Voltage at V_B selected for nonlinear separations						
16	1900	104.6	56.4	56.6	47.0	47.2
17	2000	99.9	54.1	55.0	44.0	44.9
18	2100	95.6	51.9	53.8	41.0	42.8
19	2200	91.7	49.9	53.0	37.8	40.8
20	2300	88.1	48.2	53.3	33.9	39.0
21	2400	84.8	46.5	56.8	27.1	37.3
22	**2500**	**81.8**	**45.0**	**50.6**	**35.8**	**30.2**
***E. coli* trapping occurs here**						

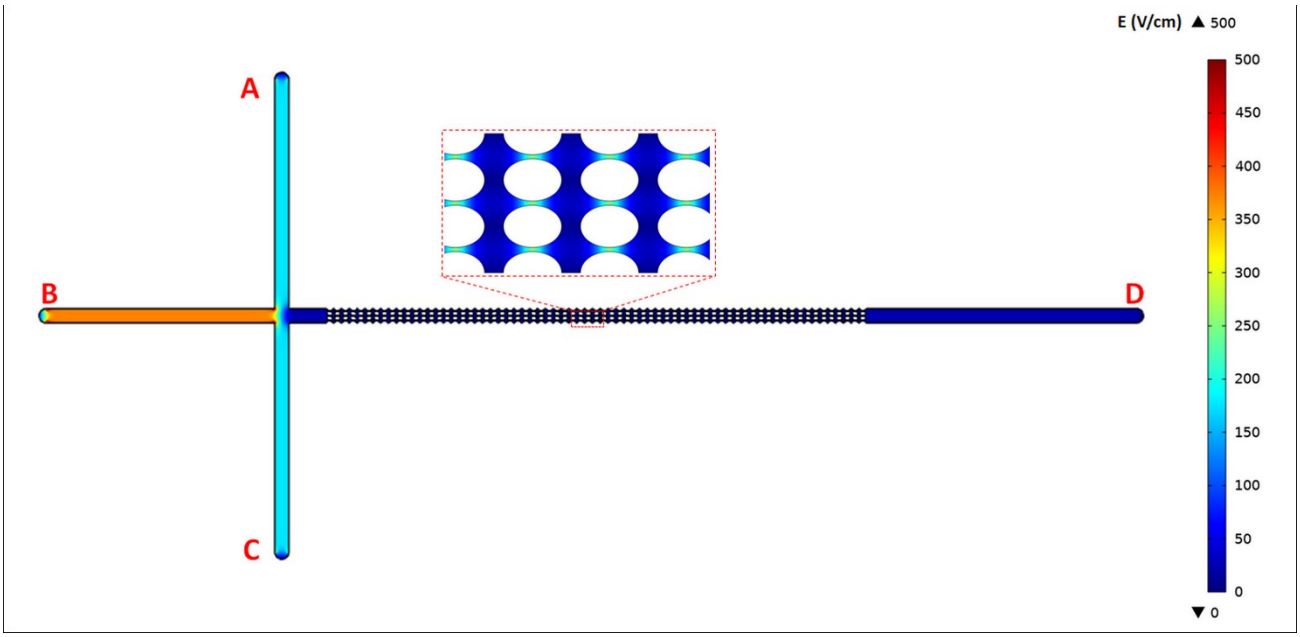

Figure S3. Electric field distribution for the selected voltages for linear separations (V_A = 100 V, V_B = 700 V, V_C = 100 V, and V_D = 0 V) with the scale for the distribution ranging between 0 to 500 V/cm. The inset shows the distribution of electric field at the post array. The average electric field computed at the vertical constriction between the posts is 194.3 V/cm.

S5. Contributions of individual EK phenomena towards the overall velocity of the particles (includes Figure S4):

Based on the voltages input into the power supply for the linear and nonlinear separations (voltages included in **Table 2**), velocity profiles were computed for each of the three analytes and the contributions of all four EK phenomena towards the overall particle velocity across the cutline shown in **Figure S2** is shown in **Figure S4**. To generate these values, the equations included in the theory section were utilized. This figure includes the velocity profiles for the separations at 194.3 V/cm and 430.4 V/cm, as well as the predicted trapping behavior of E. coli in the streaming-trapping separation at 580.6 V/cm.

As evident from the cursory observations from the flat lines near x- axis for the EP_{NL} and DEP contributions for all analytes in the separation at electric field strength of 194.3 V/cm as well as that of φKZ in other separations, the influence of EPNL and DEP towards overall particle velocity were minimal. However, for the separations at 430.4 V/cm and 580.6 V/cm, *E. coli* cells experience a significant increase in the EP_{NL}'s contribution towards overall particle velocity which indicate that they operate under nonlinear regime. Additionally, it is also interesting to note that the overall velocity profile dips below zero for *E. coli* cells at 580.6 V/cm indicating trapping of *E. coli* cells.

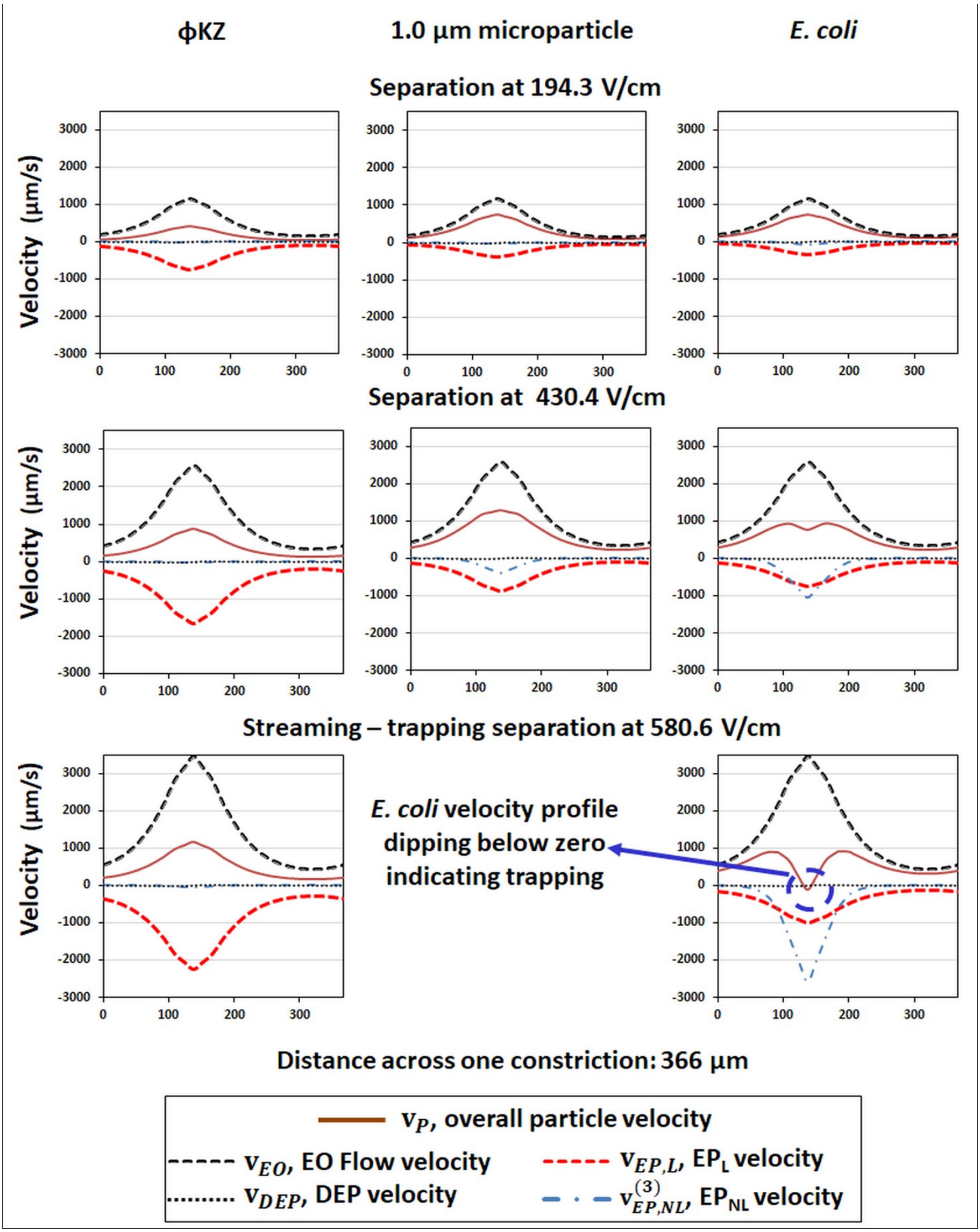

Figure S4. Velocity profiles for the analytes in the study with each individual EK phenomena's contribution towards the overall velocity (brown solid line) mapped across the cutline shown in **Figure S2** for electric field strengths of 194.3 V/cm, 430.4 V/cm and 580.6 V/cm.

S6. Elution behavior and streaming separations (includes Videos S1–S4):

The following videos record the elution behavior of the analytes at the interrogation window, demonstrating the respective peak shapes, migration speeds, and the field-induced agglomeration of the bacteriophages.

Video S1. Binary separation of bacteriophage ϕKZ (green) and microparticles P1 (red) in the streaming electrokinetic regime at an applied electric field of 194.3 V/cm.

Video S2. Binary separation of bacteriophage ϕKZ (green) and microparticles P1 (red) in the streaming electrokinetic regime at an applied electric field of 430.4 V/cm.

Video S3. Binary separation of bacteriophage ϕKZ (green) and *E. coli* cells (red) in the streaming electrokinetic regime at an applied electric field of 194.3 V/cm.

Video S4. Binary separation of bacteriophage ϕKZ (green) and *E. coli* cells (red) in the streaming electrokinetic regime at an applied electric field of 430.4 V/cm

References

1 O. Schnitzer and E. Yariv, Nonlinear electrophoresis at arbitrary field strengths: Small-Dukhin-number analysis, *Phys. Fluids*, 2014, **26**, 122002.

2 O. Schnitzer, R. Zeyde, I. Yavneh and E. Yariv, Weakly nonlinear electrophoresis of a highly charged colloidal particle, *Phys. Fluids*, 2013, **25**, 052004.

3 R. Cobos and A. S. Khair, Nonlinear electrophoretic velocity of a spherical colloidal particle, *J. Fluid Mech.*, 2023, **968**, A14.